

Cite this: DOI: 00.0000/xxxxxxxxxx

A catechol-chitosan-based adhesive and injectable hydrogel resistant to oxidation and compatible with cell therapy †

Capucine Guyot^{a,b}, Atma Adoungotchodo^{a,b}, Werner Taillades^b, Marta Cerruti^c and Sophie Lerouge^{*a,b}Received Date
Accepted Date

DOI: 00.0000/xxxxxxxxxx

Injectable hydrogels designed for cell therapy need to be adhesive to the surrounding tissues to maximize their retention and the communication between the host and the encapsulated cells. Catechol grafting is an efficient and well-known strategy to improve the adhesive properties of various polymers, including chitosan. However, catechols groups are also known to be cytotoxic as they oxidize into quinones in alkaline environments. Usually, hydrogels made from catechol-grafted chitosan (cat-CH) oxidize quickly, which tends to limit adhesion and prevent cell encapsulation. In this work, we limited oxidation and improved the cytocompatibility of cat-CH hydrogels by grafting chitosan with dihydroxybenzoic acid (DHBA), a small cat-bearing molecule known to have a high resistance to oxidation. We show that DHBA-grafted CH (dhba-CH) oxidized significantly slower and to a lesser extent than cat-CH made with hydrocaffeic acid (hca-CH). By combining dhba-CH with sodium bicarbonate and phosphate buffer, we fabricated thermosensitive injectable hydrogels with higher mechanical properties, quicker gelation and significantly lower oxidation than previously designed cat-CH systems. The resulting gels are highly adhesive on inorganic substrates, and support L929 fibroblast encapsulation with high viability ($\geq 90\%$ after 24 hours), something that was not possible in any previously designed cat-CH gel system. These properties make the dhba-CH hydrogels excellent candidates for minimally invasive and targeted cell therapy in applications that require high adhesive strength.

1 Introduction

With the unprecedented progress made in tissue engineering and cell therapy comes the need for injectable and cell-loaded scaffolds as tools to perform minimally invasive and localized therapies. To encourage both survival and growth of the encapsulated cells, these scaffolds must have adequate mechanical properties and be highly biocompatible. They should also be adhesive to increase in-situ retention, bind to surrounding tissues and facilitate the communication between the host and the cells thanks to a more intimate contact.¹ To this day, few systems combine all those required properties at once. Hydrogels, which are highly hydrated polymeric networks that mimic the extracellular ma-

trix, have been thoroughly investigated as potential answers.^{1,2} Although some very promising designs have been reported, the main challenge of biological adhesion remains: in the body, the presence of water impedes the formation of strong interactions between scaffolds and tissues.³

The marine mussels have inspired one of the most popular biomimetic approaches to create hydrogels that adhere in a wet environment. The mussel foot, which is composed of attachment plaques and threads, is remarkably adhesive to various surfaces underwater.⁴ The plaques are made of adhesive proteins known as mussel foot proteins (mfp); the most adhesive ones, mfp-3 and mfp-5,⁵ contain large amounts of the amino acid DOPA^{6,7} which includes in its structure a diphenol commonly known as catechol (cat) (Fig. 1A). Catechol plays a major and two-fold role in mussel adhesion.⁸ On the outside layer of the plaque, catechol serves an adhesive purpose and binds to surfaces through multiple weak interactions such as hydrogen bonding, electrostatic interactions and π - π coordination.⁹ In the core of the plaque, catechol has a cohesive purpose and is oxidated into a highly reactive quinone (Fig. 1C) that self-crosslinks the mfp to reinforce bulk cohesion.¹⁰ Catechol can be grafted to most polymers

^a Department of Mechanical Engineering, Ecole de technologie supérieure (ETS), 1100 Notre-Dame W Street, Montreal, QC H3C 1K3, Canada. Tel: +1 514 396-8836 ; E-mail: sophie.lerouge@etsmtl.ca

^b Centre de Recherche du CHUM, 900 Saint-Denis Street, Montreal, QC H2X 0A9, Canada

^c Department of Mining and Materials Engineering, McGill University, 3610 University Street, QC H3A 0C5, Canada

† Electronic Supplementary Information (ESI) available: [details of any supplementary information available should be included here]. See DOI: 00.0000/00000000.

through the use of a cat-bearing molecule that wears a compatible functional group, typically 3,4-dihydroxycinnamic acid (caffeic acid), dopamine, or DOPA itself.^{11–14} Cat-grafted polymers see a substantial improvement in their adhesive properties compared to their non-grafted counterparts.¹⁵ Similarly to what happens within the mussel core, cat-grafted polymers can be gelled through partial oxidative crosslinking of their catechol groups.¹⁶ Yet, catechol oxidation usually significantly decreases adhesion, as quinone cannot form most of the weak bonds that allow the binding of catechol to a great variety of substrates.^{8,9,17,18}

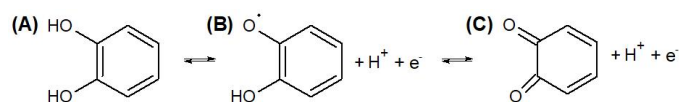


Fig. 1 Catechol (A) oxidation into semi-quinone (B) and quinone (C)

Cat-grafted polymers have been proved biocompatible for wound dressings and drug delivery applications.^{19–21} Still, numerous in-vitro studies conducted on various cells lines have underlined the cytotoxicity of both the catechol and quinone moieties.^{22–24} Many studies have correlated the observed cell apoptosis with catechol/quinone redox reactions; in particular, catechol oxidation occurs in the presence of strong oxidants such as NaIO_4 or spontaneously at a pH above 7.^{25,26}

A few strategies have been investigated to prevent catechol oxidation. One of them is working at $\text{pH} < 7$, since low pH prevents the transformation of catechols to quinones^{27,28}. However, this is not compatible with cell encapsulation where a physiological pH is crucial to ensure high cell viability. Other strategies working at physiological pH include chemical modifications: both boronate-cat complexation^{29,30} and thiourea functionalization³¹ succeeded in keeping the catechols intact during grafting. Nonetheless, deprotecting the catechols through further chemical reactions might not be readily doable after gelation or even compatible with cell encapsulation.

Among all available polymers, chitosan (CH), a highly biocompatible and biodegradable polysaccharide derived from chitin, is a very promising candidate to make cell-loaded hydrogels.³² Chitosan can be mixed with weak bases to form thermosensitive, injectable, physical hydrogels with physiological pH.^{33,34} We showed that a combination of NaHCO_3 (sodium bicarbonate) and a pH8 buffer of $\text{HPO}_4^{2-}/\text{H}_2\text{PO}_4^-$ (phosphate buffer, PB) allows to make cell-compatible hydrogels with fast gelation and high mechanical properties.^{35,36} Nonetheless, chitosan is only mildly adhesive.³⁷ Catechol can be grafted to chitosan to make catechol-chitosan (cat-CH) with improved adhesive properties.³⁸ A commonly used cat-bearing molecule for CH is 3,4-dihydroxycinnamic acid (hydrocaffeic acid, HCA) (Fig. 2A).^{39,40} HCA is sensitive to auto-oxidation and HCA-grafted CH (hca-CH) readily oxidizes at $\text{pH} \geq 7$, crosslinking the network.^{41,42} Alternatively, hca-CH can be combined with genipin⁴³ or poloxamer⁴⁴ to make injectable and adhesive hydrogels, but their gelation is slow (>60 min) and they have a low mechanical cohesiveness. Using NaHCO_3 to induce the physical gelation of hca-CH has been shown to improve to some extent the

mechanical properties and gelation kinetic of the hydrogels, but only when the catechol content was below 3%.²⁸ This limitation was attributed to the steric hindrance introduced in the network by HCA. Besides, cell compatibility might be limited since rapid oxidation was observed for all aforementioned hca-CH hydrogels.

In this work, our primary objective was to design cat-CH hydrogels that could be both highly adhesive and compatible with cell encapsulation. Both properties could be achieved at once by decreasing catechol auto-oxidation as long as the method did not induce more cytotoxicity. Here, our strategy was to replace the commonly used cat-bearing molecule HCA with dihydroxybenzoic acid (DHBA) (Fig. 2A&B). We hypothesized that in alkaline conditions, DHBA-grafted chitosan (dhba-CH) would resist oxidation better than hca-CH; in particular, (2,3)-DHBA is known to resist oxidation to a greater extent than (3,4)-DHBA.⁴⁵ The rate of catechol auto-oxidation and its dependency on the pH is related to electronic delocalization. Electron donating groups (EDG) tend to make catechol more vulnerable to oxidation while electron withdrawing groups (EWG) can increase resistance to oxidation up to pH 12.^{45,46} In HCA, the catechol is separated from the carboxylic acid by a two carbon-saturated chain that behaves like an alkyl substituent (EDG). In DHBA, however, the carboxylic acid is directly substituting the catechol; during grafting, it is replaced by an amide group (EWG).

Because DHBA is smaller than HCA, we also hypothesized that using DHBA instead of HCA could limit the steric hindrance caused by catechol grafting. Therefore, we could decrease the amount of energy required to overcome steric repulsion between the chitosan chains and, in turn, quicken gelation. We also hypothesized that because of the greater proximity between the chains, the network of dhba-CH hydrogels would be more cohesive than that of hca-CH gels, which would lead to better mechanical properties. We also used chitosan grafted with dihydrobenzaldehyde (DHB, Fig. 2C) as a control for highly oxidized hydrogels. Although almost identical to DHBA, DHB is linked to CH with an amino group (EDG) that is even more activating than an alkyl group.

To verify these hypotheses and achieve our goals, we synthesized dhba-CH and fabricated dhba-CH hydrogels. We compared the level of oxidation, mechanical properties and gelation kinetics of the dhba-CH gels with those of hca-CH and dhb-CH hydrogels. Then, after selecting the most promising formulations, we evaluated their adhesive properties and compatibility with cell encapsulation. All formulations were physically crosslinked with either NaHCO_3 or a mix of NaHCO_3 and PB to make fast-gelling thermosensitive hydrogels without using chemical crosslinkers.

2 Experimental Section

2.1 Grafting cat-bearing molecules to chitosan

2.1.1 Reagents.

Chitosan (CH) (ChitoClear™) was purchased from Primex (Island) in two batches. Its molecular weight (Mw) and degree of deacetylation (ddA) were re-evaluated following purchase. The Mw was assessed by Gel Permeation Chromatography at 160 ± 1 kDa (N=3). The ddA was es-

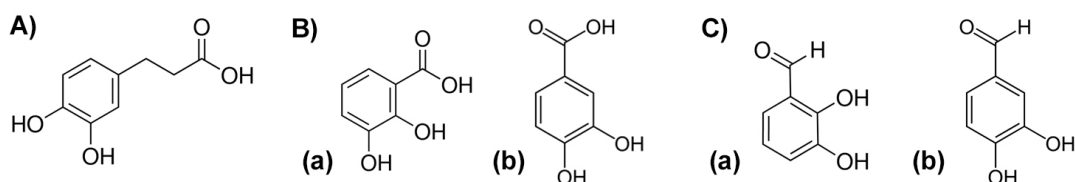


Fig. 2 Different cat bearing molecules used in this study: A) hydrocaffeic acid (HCA); B) dihydroxybenzoic acid (DHBA) and C) dihydrobenzaldehyde (DHB). Both DHBA and DHB exist in two conformations, namely 2,3 (a) and 3,4 (b).

timated at $76 \pm 4\%$ ($N=15$) by ^1H NMR (Varian VNMRS 500 MHz).⁴⁷ Hydrocaffeic acid (HCA), 2,3 dihydroxybenzoic acid (2,3-DHBA), 3,4-dihydroxybenzoic acid (3,4-DHBA), 2,3-dihydrobenzaldehyde (2,3-DHB), 3,4-dihydrobenzaldehyde (3,4-DHB), N-Ethyl-N'-(3-dimethylaminopropyl) carbodiimide (EDC), N-hydroxysuccinimide (NHS), MES hydrate, sodium periodate (NaIO_4) and sodium borohydrate (NaBH_4) were purchased from Sigma and were of analytical grade. 1M MES buffer was prepared at pH 5.5 by diluting MES hydrate in deionized water (DW). 1X phosphate buffer saline (PBS) was prepared by diluting 10X commercial PBS in DW. DMEM was from Gibco (DMEM/F-12, GlutaMAX™ supplement, Gibco, CAT 10565018).

2.1.2 Method A: synthesis of hca-CH and dhba-CH by carbodiimide coupling.

Carbodiimide coupling (Method A) is a common technique for cat-CH synthesis. This method is designed for cat-bearing molecules such as HCA and DHBA bearing a carboxylic acid. An already published protocol²⁸ was used for HCA grafting (Method A-1); briefly, CH (1% w/v) was dissolved in HCl 0.1M (pH=2). HCA (1:1 molar ratio to CH) and EDC (1:1 molar ratio to CH for hca3-CH, 2:1 for hca6-CH) were dissolved in an isovolumetric EtOH/DW solution before being added to CH. The pH was set to 4.6 and the reaction took place overnight. For DHBA, another protocol adapted from previously published work^{48,49} was created (Method A-2): CH (1% w/v) was dissolved in 0.1M HCl and the pH was raised to 5.5 before adding DHBA at either a 1.6:1 or a 3.2:1 molar ratio to CH. In parallel, EDC (2.75:1 molar ratio to CH) was dissolved in an isovolumetric EtOH/DW solution before being added dropwise to the CH/DHBA mixture. The reaction was vigorously stirred (800 rpm) at room temperature (RT) for 1 h while the pH was maintained at 5 with NaOH 1M (some samples were made at pH 6 to increase the grafting degree further). All samples from Methods A were purified by dialysis against 0.1M HCl/10 mM NaCl (2 days) followed by DW (6 h). The products were freeze-dried for 4 days before storage to avoid any leftover moisture in the samples. Method A-2 was also tested with HCA.

2.1.3 Method B: synthesis of dhb-CH by reductive amination.

Reductive amination (Method B) is a method designed for cat-bearing molecules like DHB that bear an aldehyde. Method B was adapted from previously published work.⁵⁰ CH (1% w/v) was dissolved in 1% (v/v) acetic acid (AcOH), and glacial AcOH was added dropwise until reaching a pH of 5. Then, DHB (1:2

molar ratio to CH) was dissolved in a mixture of DW and EtOH (2:1 v/v) before being added to CH under vigorous stirring. After 1 h, NaBH_4 was added to the reaction until the polymer was fully precipitated (pH 8). Because this reaction generates flammable H_2 as a by-product, NaBH_4 was added slowly, stopping regularly to avoid over-pressurization. The white and flaky precipitate was subsequently filtered (pore size = 40 μm) to remove the excess of water, and 1M HCl was gradually added until full dissolution. Purification and freeze-drying were done as described in Method A.

2.2 Characterization of cat-CH

2.2.1 ^1H NMR spectroscopy.

Nuclear magnetic resonance spectroscopy of hydrogen (^1H NMR) (Varian VNMRS 500 MHz) was used to determine the degree of deacetylation (ddA) of chitosan⁴⁷ and to ascertain the success of the cat grafting ($\delta_{\text{cat}} \sim 6.5\text{-}6.7$ ppm).

2.2.2 UV-Vis spectrometry.

UV-Vis (Cary5000 Agilent) was performed on cat-CH to calculate the grafting degree (χ). The UV-Vis spectra of cat-bearing molecules show a maximum at the following wavelengths: HCA, 280 nm; DHBA, 307 nm; DHB, 265 nm. A calibration curve was first obtained for all cat-bearing molecules between 0.1 mM and 0.5 mM. The data for HCA and DHBA can be found in Fig. S3 A&B. Then, for each batch following synthesis, cat-CH was dissolved in DW (0.1% w/v) and tested at the appropriate wavelength. Subsequently, χ was calculated using Eq. (1)[†]. The calculated χ will be specified hereafter in the name of the cat-CH as a subscript of the cat-bearing molecule; for instance, dhba-CH ($\chi=2\%$) will be written dhba2-CH.

$$\chi = \frac{C_{\text{cat}} * (ddA * M_{\text{Glu}} + (1 - ddA) * M_{\text{AcGlu}})}{C_{w,\text{catCH}} - M_{\text{CBM}} * C_{\text{cat}}} \quad (1)$$

2.2.3 Oxidation.

Catechol-to-quinone oxidation triggers a change of colour from transparent to orange;⁵¹ the degree of oxidation (α_{ox}) was qualitatively approximated based on visual evaluation of the intensity

[†] where ddA is the deacetylation degree of chitosan, M_{Glu} is the molar mass of the glucosamine monomer (161 g/mol), M_{AcGlu} is the molar mass of the acetylglucosamine monomer (203 g/mol), M_{CBM} is the molar mass of the cat-bearing molecule, $C_{w,\text{catCH}}$ is the mass concentration of cat-CH and C_{cat} is the molar concentration of catechol found through the calibration curve.

of the orange. Cat-CH solutions (3.33% w/v in DW) were prepared in vials and sealed with a hermetic cap to avoid evaporation. Pictures of the bottles were taken after 1, 2, 7, and 21 days to document any colour change. Catechol auto-oxidation within cat-CH eventually leads to oxidative crosslinking and gelation at RT. A state of no-flow following tilting was therefore correlated to a high α_{ox} . Vials were tilted to assess visually the viscosity and flowability.

2.2.4 Mucoadhesive Properties.

The mucoadhesive properties of a polymer can be evaluated in different ways by studying its interactions with mucin, the protein that constitutes mucus.⁵² Here, rheology was used as an indirect method to spot differences in adhesion between hca-CH, dhba-CH and dhb-CH without the cohesive properties of the gel influencing the results. The hypothesis is that the interactions between mucin and cat-CH translate into an increase in viscosity. The protocol was adapted from previously published work.⁵³ Cat-CH was dissolved at 2% (w/v) in 0.1 M HCl for 2 h and mucin was rehydrated at 20% (w/v) in 0.1 M HCl for 4 h. Then, 0.5 mL samples of these solutions were either mixed or added separately to 0.5 mL of 0.1 M HCl (see Table 1). Frequency sweeps at 1% strain were performed on a Physica MCR301 rheometer (Anton Paar) to find a range where viscosity was independent of frequency. The working frequency of 93 s⁻¹, which had already been chosen in previous studies⁵³, happened to fall into this range (see Fig. S1). Consequently, the viscosities of cat-CH/HCl (μ_{cat-CH} , Pa.s), mucin/HCl (μ_m) and cat-CH/mucin ($\mu_{cat-CH/m}$) were measured at 93 s⁻¹ to calculate the mucoadhesion index using Eq. (2).⁵⁴

$$M_I = \frac{\mu_{cat-CH/m} - (\mu_{cat-CH} + \mu_m)}{\mu_{cat-CH} + \mu_m} * 100 \quad (2)$$

Table 1 Composition of the three types of samples prepared for mucoadhesive rheological tests to evaluate mucoadhesion.

Viscosity	Component 1 (w/v)	Component 2 (w/v)	Final composition (w/v)
μ_m	mucin 20%	0.1 M HCl	mucin 10%
μ_{cat-CH}	cat-CH 2%	0.1 M HCl	cat-CH 1%
$\mu_{cat-CH/m}$	Mucin 20%	cat-CH 2%	cat-CH 1% mucin 10%

2.3 Fabrication and characterization of cat-CH hydrogels

2.3.1 Hydrogels preparation.

Cat-CH pre-gel solutions were prepared by combining cat-CH with a gelling agent. First, cat-CH was dissolved at 3.33% (w/v) for 2 h in DW. In parallel, the gelling agents were prepared by dissolving NaHCO₃ in either DW or pH8 phosphate buffer (PB) at different concentrations (see Table 2). Then, the pre-gel solutions were made at RT by mixing cat-CH and a gelling agent at a 3:2 (v/v) ratio, using two syringes connected by a Luer Lock. The cat-CH concentration in the pre-gels solutions was 2% (w/v). Hydrogels were subsequently formed by incubating the pre-gel solutions at 37 °C. Incubation was pursued for 24 h to ensure that all formulations had reached their final mechanical properties. The pH of both pre-gel solutions and hydrogels was measured

with a Laquatwin pH-22 electrode (HORIBA, Japan). CH hydrogels were prepared as a control material, with chitosan (3.33% w/v) dissolved in 0.1M HCl and gelled with 75 mM NaHCO₃. For cell experiments, the gelling agent was NaHCO₃ dissolved in PB (see Table 2) as previous work already demonstrated high viability with this formulation.⁵⁵

2.3.2 Oxidation.

NaIO₄ was used as an oxidizing agent to trigger oxidation in cat-CH pre-gel solutions. Briefly, 0, 3 or 6 mM NaIO₄ was dissolved along NaHCO₃ before preparing the pre-gel solutions in the same fashion as previously described. Digital pictures of the pre-gel solutions were taken right after mixing and the pre-gel solutions were then left to gel at 37 °C in a 16-well plate for 24 h.

2.3.3 Mechanical Properties.

Samples for compression were prepared in cylindrical moulds (inner diameter = 1.2 mm, height = 1 cm). Compression tests were performed on a MACH-1 testing device (Biomomentum, Canada) at 100% strain/min. Because the materials have a non-linear viscoelastic behaviour, the secant modulus (i.e., the elastic modulus at a given deformation) was calculated at 30% strain based on the recorded stress. Toughness was calculated by integrating the stress/strain curve between $\epsilon = 0\%$ and the strain at ultimate stress before breakage (ultimate strain).

2.3.4 Injectability and Gelation Kinetics.

The shear-thinning behaviour of the dhba-CH pre-gel solutions was established through viscosity tests using a PP25 geometry. Injectability was confirmed by extruding the pre-gels solutions at RT through 25G needles. Time sweeps at 37 °C were performed on a Physica MRC 301 rheometer (Anton Paar) to study the increase in storage (G') modulus with time. To simulate injection at body temperature, the temperature was initially set at 22 °C for the first minute then rapidly increased to 37 °C. The test was continued for 1 hour following that.

2.3.5 Adhesion.

Glass slides were used as an inorganic substrate for adhesion tests. Pre-gel solutions (0.5 mL) made with cat-CH and NaHCO₃ dissolved in either DW or PB were spread on a glass slide, and a second slide was placed above so that the pre-gel solution became the interface between the two slides. Water was added in the bottom of each sample-holder to saturate the samples and mimic a wet environment while preventing the samples from drying. After 24 h at 37 °C, adhesion of the hydrogels was quantified with a lap shear pulling test on an Electroforce 3,200 (TA Instruments) while recording the maximum detachment force.

2.3.6 Indirect Cytotoxicity.

A first assessment of biocompatibility was performed via indirect cytotoxicity tests where murine L929 fibroblasts (ATCC) were cultivated with culture media conditioned with hydrogel extracts. To prepare the hydrogel extracts, pre-gel solutions (1 mL) were poured into a 24-well plate and incubated at 37 °C. After 24 h, 3 mL of complete media (DMEM/F-12, 10% fetal bovine serum (FBS), 1% penicillin/streptomycin (pen/strep)) was added on top

Table 2 Listing of the formulations used throughout this work. The concentrations of the gelling agents were adapted to the considered polymer following an optimization of the NaHCO₃ concentration. C_{DW} is the concentration of the gelling agents upon dissolution and C_{gel} is the concentration of the gelling agents in the pre-gel solutions. In some cases, PB was added to NaHCO₃ as gelling agent (identified as CH [PB]).

formulation		hca-CH	dhba-CH	dhba-CH [PB]	dhb-CH	CH	CH [PB]
C _{DW} (mM)	NaHCO ₃	175	200	200	125	187.5	187.5
	PB	0	0	200	0	0	25
C _{gel} (mM)	NaHCO ₃	70	80	80	50	75	75
	PB	0	0	80	0	0	10

of the hydrogels and incubation was carried out for the next 48 h. The conditioned culture media was retrieved and changed every 24 h. Then, the conditioned culture media was used for the growth of an adhered, near confluent L929 fibroblasts layer. Cell viability was assessed by measuring metabolic activity with an Alamar Blue assay. Cells cultivated with standard culture media were used as a positive control. To carry out the assay, cells were incubated with 100 μ L Resazurin at 37 °C, 5% CO₂ for 3 h. The plate was read with a spectrophotometer (excitation wavelength: 260 nm, emission wavelength: 290 nm).

2.3.7 Cell Encapsulation.

Murine fibroblasts (L929) were used at passages 3 and 4. Cells were expanded and cultured in complete media. Fibroblasts were encapsulated in dhba-CH hydrogels as follows: 0.6 mL of dhba-CH ($\chi=2$ and 4%) was first mixed with 0.2 mL of gelling agents (either NaHCO₃ or NaHCO₃ [PB]), then with 0.2 mL of cell suspension (5 million cells/mL). The final mixture was poured in 48-well plate (200 μ L/well) and left to gel at 37 °C, 5% CO₂ for 10 min. Then, 500 μ L of complete media was added on top of each well and cells were incubated in the media for 24 h. CH [PB] hydrogels were used as positive controls as they are more cell compatible than CH hydrogels. We did not use hca-CH and dhb-CH for cell encapsulation tests. Live/Dead assays were performed after 24 h to assess cell viability. Briefly, each sample was washed with PBS and incubated with serum-free media supplemented with 2 μ M ethidium homodimer-3 and 1 μ M calcein AM (LIVE/DEAD Cell imaging kit reagents, R37601, Life Technologies, Carlsbad, USA) for 45 min at 37 °C. The sample was again washed with PBS and immediately observed using an inverted fluorescent microscope (Leica DM IRB, Feasterville, USA). Cell viability was calculated as the ratio of live cells (green) to total cells number (green and red). The counting was done using the Analyze particles function in ImageJ (National Institute of Health, USA).

2.4 Statistical Analysis

All experiments were performed at least twice in triplicate ($N \geq 2$, $n \geq 6$). Statistical analysis was performed on GraphPad Prism 7.0 with either nonparametric t tests or two-way ANOVA followed by Tukey post-hoc tests. The p-value was used to express the level of statistical significance. A p-value $p < 0.05$ (*) was considered statistically significant, and $p < 0.005$ and below (***) was considered highly statistically significant.

3 Results and Discussion

3.1 Properties of cat-CH

3.1.1 Catechol grafting degree

All the results of the different synthetic routes tested in this work are presented in Table 3. Representative ¹HNMR spectra are shown in Fig. S2. Method A-1 allowed fabricating hca-CH with grafting degrees of $\chi=3\%$ and 6%, as previously published,²⁸ but this protocol only yielded $\chi \leq 1\%$ with DHBA. The two conformations of DHBA showed different reactivity: using Method A-2 with (2,3)DHBA increased χ compared to Method A-1; besides, χ also increased when increasing the pH and the quantity of reagents. However, changing methods or parameters did not make any difference for (3,4)DHBA ($\chi=1\%$ at most). Thus, we chose (2,3)-DHBA to fabricate dhba-CH up to $\chi=8\%$ and abandoned (3,4)-DHBA, which had besides been reported as less resistant to oxidation because electrons are less delocalized in this conformation.⁴⁵ While using two different protocols for HCA and DHBA made it difficult to reach the exact same χ , all were in the same range, allowing us to compare directly dhba-CH (2, 4 and 8%) to hca-CH (3 and 6%).

In parallel, Method B produced dhb-CH with a high grafting degree ($\chi \geq 20\%$). We chose the (3,4) conformation to fabricate dhb20-CH as a control for highly oxidated cat-CH. In both methods, the conformation (2,3) yielded cat-CH with a higher χ than the conformation (3,4). We attributed this to an increase in the electron-withdrawing strength of the carboxylic acid (in the case of DHBA) or the aldehyde (in the case of DHB) due to the vicinity of the hydroxyl groups.

We also tested Method A-2 with HCA. For the same pH and quantity of reagents, hca-CH reached a significantly higher χ than dhba-CH. We speculated that the longer chain of HCA acted like a grafting arm that increased the availability of the carboxylic acid, making HCA easier to graft than DHBA.

3.1.2 Mucoadhesion of cat-CH

The binding strength of a material, i.e., its overall adhesive properties, derives from the synergistic contribution of high adhesion and high cohesion.^{56,57} Here we only measured the adhesive contribution using a non-destructive rheological method to assess the mucoadhesive properties of cat-CH. Mucoadhesion is the adhesion to mucus, a gel secreted by epithelial cells that coat most tissues in the body. We monitored the change in viscosity upon mixing cat-CH and mucin together to calculate a mucoadhesion index (see part 2.2.4 in the Experimental section).

Results are presented in Fig. 3A. The mucoadhesion index of dhba-CH and hca-CH increased with χ and was therefore at-

Table 3 Summary of the χ obtained for different cat-bearing molecules, isomers, and parameters. The χ values were calculated based on UV-Vis spectrometry (see Fig. S3).

Method	cat-bearing molecule	conformation	Ratios of reagents		pH	χ (%)
			CH	cat-bearing molecule		
A-1	HCA	/	1	1	4.6	3
A-1	HCA	/	1	1	2	6
A-1	DHBA	(2,3)	1	1	4.6	≤ 1
A-2	HCA	/	1	1.6	2.75	30
A-2	DHBA	(2,3)	1	1.6	2.75	2
A-2	DHBA	(2,3)	1	1.6	2.75	4
A-2	DHBA	(2,3)	1	3.2	2.75	8
A-2	DHBA	(3,4)	1	1.6	2.75	1
A-2	DHBA	(3,4)	1	3.2	2.75	1
B	DHB	(2,3)	1	0.5	/	40
B	DHB	(3,4)	1	0.5	/	20

tributed to the increase in catechol content. Surprisingly, despite its high χ , the mucoadhesion index of dhb20-CH was comparable to that of dhba-CH and hca-CH with $\chi \leq 4\%$.

3.1.3 Oxidation of cat-CH

To compare the rate of catechol-to-quinone oxidation of the various cat-CH, we monitored their change in colour when dissolved in DW. Fig. 3B shows the pictures taken at day 1 and day 21 (see Fig. S4 for the other time points) while Fig. 3C summarizes the evolution of the oxidation degree (α_{ox}), visually evaluated based on the colour change. Immediately after dissolution, oxidation was already noticeable for hca3-CH, hca6-CH and dhba8-CH. Over the course of the experiment, the α_{ox} of dhba-CH seemed to remain unaffected regardless of χ ; however, hca-CH and dhb-CH oxidated with time. The three polymers that reached a high α_{ox} were, in order, hca6-CH (day 2), hca3-CH (day 7) and dhb20-CH (day 21). Only hca6-CH attained the point of no-flow over the course of the experiment, meaning it underwent oxidative crosslinking. As expected, a higher χ made oxidation more noticeable because of the higher catechol content.

These results confirm our main hypothesis, namely that the amide group in dhba-CH protected catechol from oxidation thanks to its electron-withdrawing effect. Conversely, catechol became more vulnerable to oxidation when substituted with an EDG such as the alkyl group in hca-CH or the amino group in dhb-CH.⁴⁵ This phenomenon had already been observed and reported for DOPA.^{58,59} The difference in oxidation rates between hca-CH and dhb-CH can be explained by the fact that hca3-CH and hca6-CH were already partially oxidized during dissolution despite their low χ . As underlined by some recent work on catechol grafting,⁴⁹ catechol oxidation had probably already started during fabrication with Method A-1.

3.2 Properties of cat-CH hydrogels with NaHCO₃

3.2.1 Oxidation of hydrogels

Dhba-CH and dhb-CH have already been synthesized and characterized in previous studies^{48,60} but have never been turned into hydrogels. After showing that substituting HCA for DHBA significantly decreased catechol auto-oxidation in cat-CH solutions, we tested whether the same effect was obtained for cat-CH hydrogels prepared with 70 mM NaHCO₃. We used CH and dhb20-CH as positive and negative controls respectively, and we com-

pared the oxidation of the pre-gel solutions and the hydrogels after 24 h of gelation at 37 °C (Fig. 4). Dhba-CH and hca-CH pre-gel solutions were all transparent like CH, suggesting that no oxidation occurred following the addition of NaHCO₃. After 24 h of gelation, we classified them by sight from the least oxidized to the most oxidized: CH<dhba2-CH<dhba4-CH<dhba8-CH<hca3-CH<<dhba20-CH. While oxidation was more noticeable when increasing χ , dhba8-CH hydrogels appeared less oxidized than hca3-CH hydrogels, suggesting that DHBA succeeded in protecting the cat group against oxidation.

To confirm our hypothesis, we also prepared dhba-CH hydrogels with NaIO₄, a potent oxidant able to quickly oxidize catechols into quinones⁶¹ (Fig. S5). The hydrogels turned yellow/orange after 24h; yet, even in the presence of 6 mM NaIO₄, the colour was less deep and intense than what we observed for the hca3-CH hydrogels without oxidants. Based on these results, we concluded that dhba-CH hydrogels were more resistant to oxidation than hca-CH hydrogels.

3.2.2 Mechanical properties and gelation kinetics

Chitosan is only soluble when its amino groups are protonated (pH ≤ 6.3). The pre-gel solutions made of chitosan and a gelling agent are liquid at room temperature, and physical gelation happens through a temperature-triggered deionization of the amino groups of chitosan.^{62,63} The nature of the gelling agent and its concentration are known to have a strong influence on the properties of the gels. When using sodium bicarbonate (NaHCO₃), previous work has shown that the stiffness of CH-based hydrogels as a function of NaHCO₃ concentration followed a bell curve, with an optimum around 70 mM for hca3-CH²⁸ and 75 mM for chitosan.³⁵ For dhba-CH with $\chi \leq 8\%$, this optimum was found at 80 mM (data not shown). Like hca-CH pre-gel solutions,²⁸ all dhba-CH pre-gel solutions were shear-thinning and injectable at 22 °C through 25G needles (Fig. S6). At high shear rates ($v \geq 10$ s⁻¹), the viscosity of the pre-gel solutions was significantly lower than that of other recently designed injectable systems ($\mu \geq 1$ Pa.s compared to $\mu \leq 0.02$ Pa.s for dhba-CH hydrogels).^{64,65}

Even at the optimised NaHCO₃ concentration of 50 mM, dhb20-CH yielded weak hydrogels (data not shown). Because DHBA and DHB have the same size and thus create the same steric hindrance at a given χ , we linked the low mechanical properties found for dhb20-CH gels to their high catechol and quinone

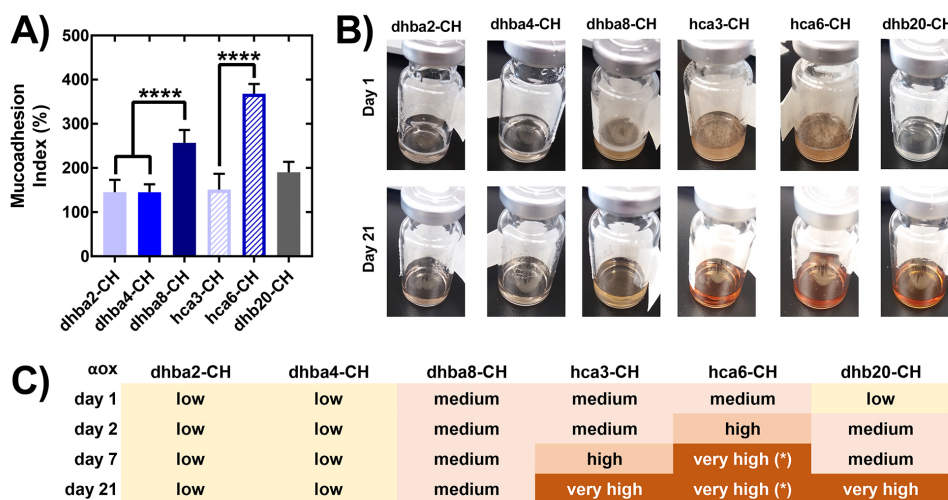
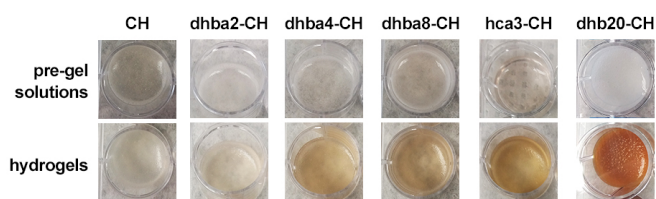


Fig. 3 Mucoadhesion and oxidation of cat-CH. A) Mucoadhesion index assessed via viscosity measurements. B) Pictures of cat-CH solutions over time. C) Summary of the evolution of the oxidation degree with time based on visual observation. (*) indicates no flow following the tilt of the bottle.



content.

Following the acquisition of the stress/strain curves (Fig. 5A), we measured the stress under compression at 30% deformation and calculated the secant modulus of the cat-CH hydrogels (Fig. 5B) to evaluate their mechanical properties. The stiffness of dhba-CH hydrogels was lower than that of CH hydrogels and decreased with increasing χ , which we attributed to the steric hindrance of DHBA causing irregularities in the network. However, at similar χ , stiffness was significantly higher for dhba-CH hydrogels than for hca-CH hydrogels ($p < 0.05$). This agreed with our hypothesis that choosing a smaller cat-bearing molecule (DHBA instead of HCA) would increase network cohesion. We calculated the toughness by integrating the stress-strain curves and found that dhba-CH hydrogels were significantly more tough than hca-CH hydrogels (Fig. 5C). Similarly, both breaking strain and stress were higher for dhba-CH hydrogels than for hca-CH hydrogels ($p < 0.05$) (Fig. S7A&B). Besides, the mechanical properties of dhba-CH hydrogels were overall superior to that values reported recently on hca10-CH hydrogels crosslinked by bio-silicification ($\sigma_{max} = 8$ kPa vs. 61 ± 7 kPa for dhba8-CH hydrogels) or by metal coacervation ($E = 5$ kPa vs. 20 ± 5 kPa for dhba8-CH hydrogels).^{66,67}

Then, to study the influence of steric hindrance on the gelation

rate at body temperature, we performed time sweep rheological tests with dhba-CH and hca-CH (1 min at 22 °C followed by 1 h at 37 °C) (Fig. 6 (a)). As illustrated by the slow increase of G' with time, hca3-CH only mildly responded to the temperature trigger. Conversely, dhba-CH with $\chi \leq 4\%$ showed a clear inflection following the switch in temperature, and reached a G' twice as high as hca3-CH after 20 min. This inflection was less visible for $\chi = 8\%$; nonetheless, the slope of G' for dhba8-CH was still greater than for hca3-CH. We thus confirmed that using DHBA over HCA decreased steric repulsion between the chains and benefited gelation altogether, bringing both faster gelation and higher mechanical properties to the resulting hydrogels. Gelation was significantly faster than other cat-CH hydrogels,⁶⁸ including recently designed hydrogels such as thermosensitive cat-CH/oyster peptide microsphere hydrogels ($G' = 1$ Pa after 12 min vs. 15 Pa for dhba4-CH hydrogels).⁶⁹

3.3 Properties of cat-CH hydrogels with PB

Even though the properties of cat-CH hydrogels were improved by reducing catechol steric hindrance, the gelation of dhba-CH with NaHCO₃ was still slow compared to that of chitosan³⁴. For in-vivo injection, quickly reaching high mechanical properties to ensure no leakage at the target site is critical.³⁶ To accelerate the gelation of dhba-CH, we used 80 mM of PB, a pH8 buffer of H₂PO₄⁻/HPO₄²⁻ (pKa = 7.2) that has been shown to speed up the gelation of CH hydrogels significantly when used in combination with NaHCO₃.³⁵ As already reported,³⁶ PB tends to increase the pH of the pre-gel solutions, increasing the risk of cat auto-oxidation as well. Due to this, as expected, adding PB to hca3-CH pre-gel solutions turned them into oxidized precipitates that were too weak for mechanical characterization. Conversely, adding PB did not alter the oxidation state of dhba-CH thanks to its higher resistance to oxidation. Therefore, we were able to characterize the gelation kinetics and mechanical properties of dhba-CH [PB] hydrogels.

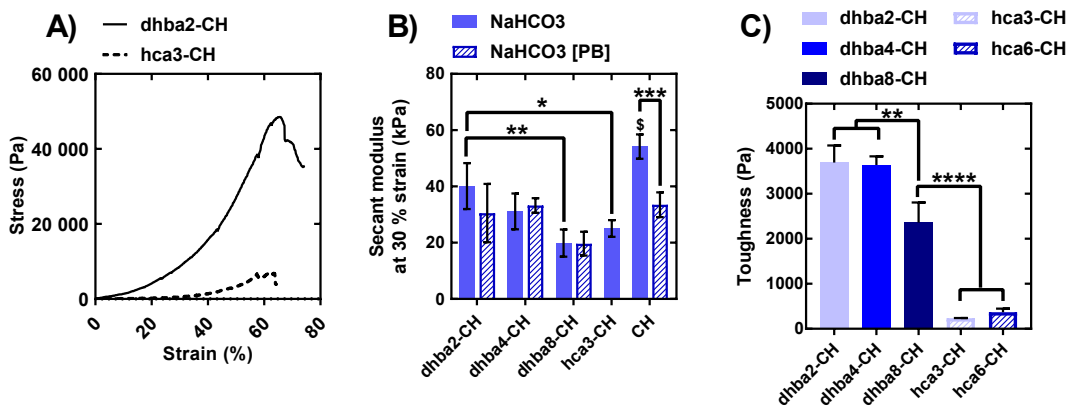


Fig. 5 A) Stress-strain compression data until breakage obtained for dhba2-CH and hca3-CH hydrogels. Rupture occurred at lower strain and lower loads for hca-CH than for dhba-CH. B) Secant modulus in compression of dhba-CH, hca-CH and CH hydrogels prepared with their optimized NaHCO₃ concentration with and without 80 mM PB (mean \pm SD of n=6, N=3; * p < 0.05; \$: statistically significant to all the other formulations). C) Toughness (Pa) of dhba-CH and hca-CH hydrogels calculated by integrating the stress-strain compression curve from 0 to breakage.

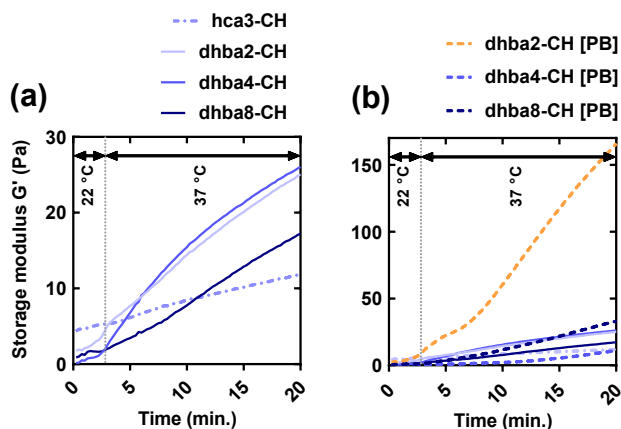


Fig. 6 Time sweeps (1 min at 22 °C followed by 1 h at 37 °C) for dhba-CH and hca-CH hydrogels (G' is the mean of N=3 and n>6) prepared with (a) the optimized NaHCO₃ concentration and (b) the addition of PB.

While PB did not affect the gelation speed of dhba-CH with $\chi \geq 4\%$, it succeeded in significantly increasing the gelation rate of dhba2-CH (Fig. 6 (b)), with G' reaching 20 Pa in 6 ± 3 min in contrast to 16 ± 4 min without PB (p < 0.05).

Previous work on chitosan hydrogels has shown that their excellent mechanical properties were granted by the slowness of the amine deionization; when gelation is accelerated, the chains are given less time to optimize their spatial organization. As such, increasing the gelation speed with PB was correlated to a loss in stiffness.³⁵ Here, contrary to CH, adding PB did not significantly affect the secant modulus of dhba-CH hydrogels (Fig. 5B). We hypothesized that catechol engaged in competing electrostatic interactions with H₂PO₄⁻ and HPO₄²⁻, preventing PB from interacting with chitosan altogether.

3.4 Adhesion of cat-CH hydrogels

Since quinones may contribute to adhesion on organic substrates through covalent bonding,^{9,70} adhesion tests were performed on inorganic substrates where quinones are known to adhere significantly less than catechols.⁷¹ We used dhba-CH hydrogels with different grafting degrees and compared them to hca3-CH and CH hydrogels. Thanks to their superior gelation speed that made them especially promising, dhba2-CH [PB] hydrogels were tested as well. We quantified hydrogel adhesion by recording the force necessary to detach the hydrogels from glass slides (Fig. 7A). All samples were gelled in a wet environment as sample-drying would artificially increase the detachment force results.

Dhba-CH hydrogels with $\chi \leq 4\%$ showed a significantly higher detachment force than CH and the other cat-CH formulations, and dhba2-CH hydrogels showed the highest values amongst all formulations (Fig. 7B). Even if the detachment force of dhba2-CH [PB] hydrogels was lower than that of dhba2-CH hydrogels, it significantly outperformed CH and hca3-CH and was comparable to other recently designed cat-CH or cat-alginate hydrogels.^{27,72}

Despite their higher cat content and better performance in mucoadhesion tests, the adhesion of dhba8-CH hydrogels to glass slides was significantly lower than that of dhba-CH gels with lower χ . Two factors come at play to explain these results. First, dhba2-CH hydrogels had shown the highest secant modulus during compression tests, and the stiffness of dhba-CH decreased with increasing grafting degree (see Fig. 5B). Because the bonding strength depends on both adhesion and cohesion, the mechanical properties may have limited the maximum detachment force. Second, we previously observed that dhba8-CH and hca3-CH hydrogels had a higher oxidation degree than dhba2-CH and dhba4-CH hydrogels, hence a higher ratio of quinones to catechols. While cat groups strongly adhere to inorganic substrates, they lose this property when oxidized into quinones. Since dhba-CH hydrogels with $\chi \leq 4\%$ had both high cohesion and low oxidation, they outperformed the other formulations.

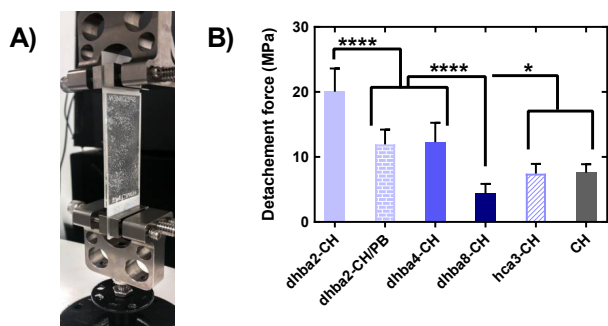


Fig. 7 A) Shear-detachment tests to evaluate cat-CH hydrogel adhesion to glass substrates. Each formulation gelled between two glass slides for 24h at 37°C in a wet environment. The slides were pulled apart at a steady rate of 1 mm/min. B) The resulting detachment force is recorded and normalized to the area of the glass slide. Unmodified chitosan (CH) hydrogels were used as controls. (mean \pm SD of $N > 2$, $n > 6$, **** $p < 0.001$)

3.5 Cytocompatibility and Cell Encapsulation

3.5.1 pH of hydrogels

We measured the pH of the hydrogels before performing indirect cytotoxicity tests; to limit cytotoxicity, the pH must stay inside the physiological range. Before adding the cells and the media, the pH of all the pre-gel solutions was close to 7 (see Fig. S8). Adding PB had a mild buffering effect on the pre-gel solutions, bringing the pH closer to physiological values (pH=7.3 for dhba2-CH [PB] hydrogels). The pH increased during gelation. For dhba-CH with $\chi \geq 4\%$, this increase was reduced in the presence of PB, probably because PB kept its buffering ability by not physically crosslinking the network.

3.5.2 Indirect cytotoxicity

Indirect cytotoxicity was evaluated on all formulations, including dhb20-CH hydrogels (control for high oxidation). L929 fibroblasts were exposed to cell culture media previously conditioned with hydrogel extracts. The metabolic activity of the cells exposed to the extracts released during the first and second day is presented in Fig. 8A. For the first day extracts, only dhba-CH hydrogels with $\chi \leq 4\%$ showed no significant cytotoxicity (viability $\geq 80\%$). Hca3-CH and hca6-CH were mildly cytotoxic. Extracts from dhb20-CH hydrogels were strongly cytotoxic (viability $\leq 40\%$) and their cytotoxicity persisted after 24h, contrary to all the other formulations ($p < 0.001$).

The cytotoxicity of cat has been reported numerous times in the literature and attributed to the generation of semi-quinone, a free radical formed during the auto-oxidation of cat^{22,73,74} (see Fig. 1B). In the presence of oxygen, these radicals can create reactive oxygen species (ROS)⁷⁵ which, in high concentrations, cause oxidative stress to cells.⁷⁶ Based on these results as well as the observed oxidation states of the hydrogels (see Fig. 4), we can infer that the observed cytotoxic effects were indeed related to cat oxidation and the subsequent production of ROS. Trapped into the network during gelation, semi-quinone could have been

transferred into the extracts. The high cytotoxicity of the dhb-CH extracts even after 24 h would thus be explained by the high χ and high oxidation levels of the dhb-CH hydrogels.

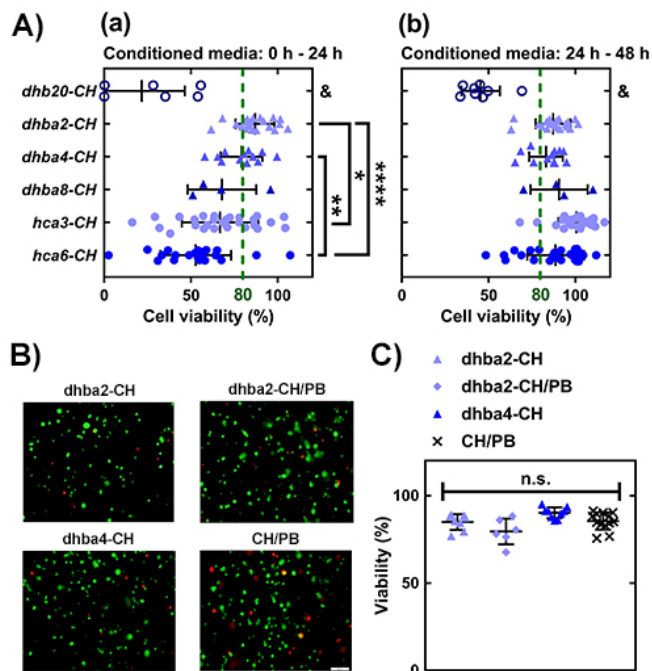


Fig. 8 A) Indirect cytotoxicity tests: Viability of L929 fibroblasts in DMEM media conditioned with different cat-CH hydrogels extracts collected in the first (a) and second day (b). Samples were declared cytotoxic when the viability was below 80%. &: statistically different from all other formulations. B) Viability of L929 fibroblasts encapsulated in dhba-CH and CH (control) hydrogels using Live/Dead assay performed after 24 h in culture. The living cells appear in green and the dead cells in red. The scale bar (on the control picture) is 200 μ m. C) Quantification of the Live-Dead Assays: no significant differences were observed between conditions in terms of cell viability.

3.5.3 Cell Encapsulation

We encapsulated L929 fibroblasts in the most promising formulations, namely dhba2-CH, dhba2-CH [PB] and dhba4-CH hydrogels, selected for their high adhesive properties and low cytotoxicity. Cell viability was assessed after 24 h of incubation using Live-dead staining. As shown in Fig. 8B&C, all the tested formulations showed a high number of living cells (viability $> 80\%$) without any significant difference between dhba-CH hydrogels and the control (CH [PB] hydrogels). Based on this, we concluded that the presence of catechol in these three formulations did not induce any significant cytotoxicity.

To our knowledge, this is the first report of cat-based hydrogels that are both injectable and compatible with cell encapsulation. For instance, hydrogels based on oxidized cat-PEG,⁷⁷ cat-alginate⁷⁸ and cat-hyaluronic acid (cat-HA)⁷⁹⁻⁸¹ are cytocompatible despite being formed through oxidative crosslinking; however, they either need to be gelled in vitro beforehand or to be directly painted on the tissue, restricting their use to invasive procedures. Conversely, other injectable cat-based hydrogels like cat-aldehyde-modified-alginate²⁷, thermosensitive quat-

ernized cat-CH⁶⁴, pH-responsive cat-CH/oxidized-pullulan⁸² or photo-crosslinkable Fe-cat-methacrylated CH⁸³ hydrogels have been designed for drug delivery and wound dressing applications. Their cytotoxicity has only been evaluated via indirect or co-culture contact tests, and they have no proven compatibility with cell encapsulation. Thus, the dhba-CH [PB] hydrogels are the first example of injectable cat-CH hydrogels that are not only cytocompatible but also possible to use as cell-loaded vehicles to perform targeted cell therapy.

4 Conclusions

In this paper, we showed that by carefully selecting the cat-bearing molecule and the catechol grafting degree, we succeeded in fabricating a hydrogel that is both adhesive and compatible with cell encapsulation. Choosing a cat-bearing molecule substituted by an EWG such as DHBA significantly decreased catechol oxidation in cat-CH, which in turn allowed for the preparation of mechanically strong and adhesive hydrogels. This strategy is much simpler than previously reported catechol protection strategies through chemical modification.

While cat-CH prepared with DHB or HCA and combined with NaHCO₃ led to oxidized and non-cohesive hydrogels, cat-CH hydrogels prepared with up to 8% DHBA resisted oxidation at physiological pH. Dhba-CH hydrogels with $\chi \leq 4\%$ showed very low indirect cytotoxicity and excellent cell viability after 24 h of encapsulation. Thanks to the low steric hindrance of DHBA, they also showed higher cohesion and faster gelation than previously reported hca-CH hydrogels.

The hydrogels made with dhba2-CH, NaHCO₃ and PB combined all the desired properties at once, with a quicker gelation and higher cohesion than many other cat-CH hydrogels. This injectable and adhesive hydrogel could be an excellent candidate in many tissue regeneration applications, such as cartilage regeneration or cardiac tissue repair.⁸⁴ Future work will include ex-vivo shear detachment tests to demonstrate the adhesion on biological tissues, as well as cell viability and proliferation assays on longer time scales. In-vivo tests will be also necessary to confirm the effective transfer of the encapsulated cells and their secreted factors to the surrounding tissues.

Conflicts of interest

There are no conflicts to declare.

Acknowledgements

We thank Tommy Malaret (ETS) for performing the Alamar blue assays, Michael Dubois (ETS) for the use of the freeze-drier and Robin Stein (McGill University) for the training in ¹HNMR spectrometry. This work was funded by the Fonds de recherche du Québec Nature et technologies (FRQNT) (Grant number: 2016-PR-191243 and Doctoral Research Scholarship B2X); the NSERC (Discovery Grant), and the CRC in Biosynthetic Interfaces.

Notes and references

1 D. Seliktar, *Science*, 2012, **336**, 1124–1128.

2 N. A. Peppas and J. J. Sahlin, *Biomaterials*, 1996, **17**, 1553–1561.

- 3 G. P. Maier, M. V. Rapp, J. H. Waite, J. N. Israelachvili and A. Butler, *Science*, 2015, **349**, 628–632.
- 4 H. Lee, N. F. Scherer and P. B. Messersmith, *Proceedings of the National Academy of Sciences*, 2006, **103**, 12999–13003.
- 5 E. W. Danner, Y. Kan, M. U. Hammer, J. N. Israelachvili and J. H. Waite, *Biochemistry*, 2012, **51**, 6511–6518.
- 6 J. H. Waite and M. L. Tanzer, *Science*, 1981, **212**, 1038–1040.
- 7 H. Zhao and J. H. Waite, *Journal of Biological Chemistry*, 2006, **281**, 26150–26158.
- 8 M. Yu and T. T. J. Deming, *Macromolecules*, 1998, **31**, 4739–45.
- 9 J. Saiz-Poseu, J. Mancebo-Aracil, F. Nador, F. Busqué and D. Ruiz-Molina, *Angewandte Chemie International Edition*, 2019, **58**, 696–714.
- 10 T. Priemel, R. Palia, M. Babych, C. J. Thibodeaux, S. Bourgault and M. J. Harrington, *Proceedings of the National Academy of Sciences of the United States of America*, 2020, **117**, 7613–7621.
- 11 A. O. Aytekin, S. Morimura and K. Kida, *Journal of Bioscience and Bioengineering*, 2011, **111**, 212–216.
- 12 Y. Lee, H. J. Chung, S. Yeo, C.-H. Ahn, H. Lee, P. B. Messersmith and T. G. Park, *Soft Matter*, 2010, **6**, 977.
- 13 J. Liu, S. Liu, Y. Chen, L. Zhang, J. Kan and C. Jin, *Food hydrocolloids*, 2017, **71**, 176–186.
- 14 J. H. Waite, *Nature Materials*, 2008, **7**, 8–9.
- 15 K. Zhang, Z. Wei, X. Xu, Q. Feng, J. Xu and L. Bian, *Materials Science and Engineering C*, 2019, **103**, 109835.
- 16 W. Y. Quan, Z. Hu, H. Z. Liu, Q. Q. Ouyang, D. Y. Zhang, S. D. Li, P. W. Li and Z. M. Yang, *Molecules*, 2019, **24**, 1–27.
- 17 B. K. Ahn, *Journal of the American Chemical Society*, 2017, **139**, 10166–10171.
- 18 A. H. Hofman, I. A. van Hees, J. Yang and M. Kamperman, *Advanced Materials*, 2018, **30**, 1704640.
- 19 J. Li, A. D. Celiz, J. Yang, Q. Yang, I. Wamala, W. Whyte, B. R. Seo, N. V. Vasilyev, J. J. Vlassak, Z. Suo and D. J. Mooney, *Science (New York, N.Y.)*, 2017, **357**, 378–381.
- 20 J. Su, F. Chen, V. L. Cryns and P. B. Messersmith, *Journal of the American Chemical Society*, 2011, **133**, 11850–11853.
- 21 Y. Xu, J. Han and H. Lin, *Carbohydrate Polymers*, 2017, **156**, 372–379.
- 22 T. J. Monks, R. P. Hanzlik, G. M. Cohen, D. Ross and D. G. Graham, *Toxicology and Applied Pharmacology*, 1992, **112**, 2–16.
- 23 P. J. O'Brien, *Chemico-Biological Interactions*, 1991, **80**, 1–41.
- 24 J. Yang, M. A. Cohen Stuart and M. Kamperman, *Chemical Society Reviews*, 2014, **43**, 8271–8298.
- 25 A. Nemeikaite-Čeniene, A. Imbrasaitė, E. Sergediene and N. Čenas, *Archives of Biochemistry and Biophysics*, 2005, **441**, 182–190.
- 26 N. Schweigert, A. J. Zehnder and R. I. Eggen, *Environmental Microbiology*, 2001, **3**, 81–91.
- 27 S. Yan, W. Wang, X. Li, J. Ren, W. Yun, K. Zhang, G. Li and J. Yin, *Journal of Materials Chemistry B*, 2018, **6**, 6377–6390.

- 28 C. Guyot, M. Cerruti and S. Lerouge, *Materials Science and Engineering: C*, 2020, **118**, 111529.
- 29 A. R. Narkar, B. Barker, M. Clisch, J. Jiang and B. P. Lee, *Chemistry of Materials*, 2016, **28**, 5432–5439.
- 30 A. Schneider, J. Hemmerlé, M. Allais, J. Didierjean, M. Michel, M. D'Ischia and V. Ball, *ACS Applied Materials and Interfaces*, 2018, **10**, 7574–7580.
- 31 Y. J. Xu, K. Wei, P. Zhao, Q. Feng, C. K. K. Choi and L. Bian, *Biomaterials Science*, 2016, **4**, 1726–1730.
- 32 M. Rinaudo, *Progress in Polymer Science*, 2006, **31**, 603–632.
- 33 A. Chenite, C. Chaput, D. Wang, C. Combes, M. Buschmann, C. D. Hoemann, J. C. Leroux, B. Atkinson, F. Binette and A. Selmani, *Biomaterials*, 2000, **21**, 2155–2161.
- 34 L. Liu, X. Tang, Y. Wang and S. Guo, *International Journal of Pharmaceutics*, 2011, **414**, 6–15.
- 35 E. Assaad, M. Maire and S. Lerouge, *Carbohydrate Polymers*, 2015, **130**, 87–96.
- 36 C. Ceccaldi, E. Assaad, E. Hui, M. Buccionyte, A. Adoungotchodo and S. Lerouge, *Macromolecular Bioscience*, 2017, **17**, 1600435.
- 37 V. Grabovac, D. Guggi and A. Bernkop-Schnürch, *Advanced Drug Delivery Reviews*, 2005, **57**, 1713–1723.
- 38 T. M. M. Ways, W. M. Lau and V. V. Khutoryanskiy, *Polymers*, 2018, **10**, 267.
- 39 K. Kim, K. Kim, J. H. Ryu and H. Lee, *Biomaterials*, 2015, **52**, 161–170.
- 40 G. M. Soliman, Y. L. Zhang, G. Merle, M. Cerruti and J. Barralet, *European Journal of Pharmaceutics and Biopharmaceutics*, 2014, **88**, 1026–1037.
- 41 K. Kim, J. H. Ryu, Y. Lee and H. Lee, *Biomaterials Science*, 2013, **1**, 783–790.
- 42 J. Xu, G. M. Soliman, J. Barralet and M. Cerruti, *Langmuir*, 2012, **28**, 14010–14017.
- 43 J. Xu, *PhD thesis*, McGill University, 2015.
- 44 J. H. Ryu, Y. Lee, W. H. Kong, T. G. Kim, T. G. Park and H. Lee, *Biomacromolecules*, 2011, **12**, 2653–2659.
- 45 G. P. Maier, C. M. Bernt and A. Butler, *Biomaterials Science*, 2018, **6**, year.
- 46 M. T. Smith, C. G. Evans, H. Thor and S. Orrenius, *Oxidative Stress*, 1985, 91–113.
- 47 M. Lavertu, Z. Xia, A. Serreqi, M. Berrada, A. Rodrigues, D. Wang, M. Buschmann and A. Gupta, *Journal of Pharmaceutical and Biomedical Analysis*, 2003, **32**, 1149–1158.
- 48 J. Liu, C. Guang Meng, Y. Hua Yan, Y. Na Shan, J. Kan and C. Hai Jin, *International Journal of Biological Macromolecules*, 2016, **89**, 518–526.
- 49 A. R. Narkar, E. Cannon, H. Yildirim-Alicea and K. Ahn, *Langmuir*, 2019, **35**, 16013–16023.
- 50 P. S. Yavvari and A. Srivastava, *Journal of Materials Chemistry B*, 2015, **3**, 899–910.
- 51 J. H. Ryu, S. Hong and H. Lee, *Acta Biomaterialia*, 2015, **27**, 101–115.
- 52 J. B. da Silva, S. B. d. S. Ferreira, A. V. Reis, M. T. Cook and M. L. Bruschi, *Polymers*, 2018, **10**, 254.
- 53 E. E. Hassan and J. M. Gallo, *Pharmaceutical Research: An Official Journal of the American Association of Pharmaceutical Scientists*, 1990, **7**, 491–495.
- 54 A. Graça, L. M. Gonçalves, S. Raposo, H. M. Ribeiro and J. Marto, *Pharmaceutics*, 2018, **10**, 110.
- 55 A. Monette, C. Ceccaldi, E. Assaad, S. Lerouge and R. Lapointe, *Biomaterials*, 2016, **75**, 237–249.
- 56 J. Yang, R. Bai, B. Chen and Z. Suo, *Advanced Functional Materials*, 2020, **30**, 1901693.
- 57 W. Zhu, Y. J. Chuah and D. A. Wang, *Acta Biomaterialia*, 2018, **74**, 1–16.
- 58 A. N. Basma, E. J. Morris, W. J. Nicklas and H. M. Geller, *Journal of Neurochemistry*, 1995, **64**, 825–832.
- 59 Y. Z. Zhou, R. G. Alany, V. Chuang and J. Wen, *Chromatographia*, 2012, **75**, 597–606.
- 60 A. Clifford, X. Pang and I. Zhitomirsky, *Colloids and Surfaces A: Physicochemical and Engineering Aspects*, 2018, **544**, 28–34.
- 61 J. Yang, V. Saggiomo, A. H. Velders, M. A. Cohen Stuart and M. Kamperman, *PLoS ONE*, 2016, **11**, 1–17.
- 62 J. Cho, M. C. Heuzey, A. Bégin and P. J. Carreau, *Biomacromolecules*, 2005, **6**, 3267–3275.
- 63 M. Lavertu, D. Filion and M. Buschmann, *Biomacromolecules*, 2008, **9**, 640–650.
- 64 Z. Zheng, S. Bian, Z. Li, Z. Zhang, Y. Liu, X. Zhai, H. Pan and X. Zhao, *Carbohydrate Polymers*, 2020, **249**, 116826.
- 65 P. Karami, N. Nasrollahzadeh, C. Wyss, A. O'Sullivan, M. Broome, P. Procter, P. Bourban, C. Moser and D. P. Pioletti, *Macromolecular Rapid Communications*, 2021, 2000660.
- 66 J. N. Kim, J. Lee, H. Lee and I. K. Oh, *Nano Energy*, 2021, **82**, 105705.
- 67 S. H. Hong, J. H. Ryu and H. Lee, *Journal of Industrial and Engineering Chemistry*, 2019, **79**, 425–430.
- 68 J. Xu, M. Tam, S. Samaei, S. Lerouge, J. Barralet, M. M. Stevenson and M. Cerruti, *Acta Biomaterialia*, 2017, **48**, 247–257.
- 69 D. Zhang, Q. Ouyang, Z. Hu, S. Lu, W. Quan, P. Li, Y. Chen and S. Li, *International Journal of Biological Macromolecules*, 2021, **173**, 591–606.
- 70 D. Zhou, S. Li, M. Pei, H. Yang, S. Gu, Y. Tao, D. Ye, Y. Zhou, W. Xu and P. Xiao, *ACS Applied Materials and Interfaces*, 2020, **12**, 18225–18234.
- 71 W. Wei, J. Yu, C. Broomell, J. N. Israelachvili and J. H. Waite, *Journal of the American Chemical Society*, 2013, **135**, 377–383.
- 72 R. Xu, S. Ma, Y. Wu, H. Lee, F. Zhou and W. Liu, *Biomaterials Science*, 2019, **7**, 3599–3608.
- 73 G. Barreto, D. Madureira, F. Capani, L. Aon-Bertolino, E. Saraceno and L. D. Alvarez-Giraldez, *Environmental and Molecular Mutagenesis*, 2009, **50**, 771–780.
- 74 M. R. G. Pereira, E. S. de Oliveira, F. A. G. A. de Villar, M. S. Grangeiro, J. Fonseca, A. R. Silva, M. d. F. D. Costa, S. L. Costa and R. d. S. El-Bachá, *Jornal Brasileiro de Patologia e Medicina Laboratorial*, 2004, **40**, 280–285.
- 75 H. Meng, Y. Li, M. Faust, S. Konst and B. P. Lee, *Acta Biomate-*

- rialia*, 2015, **17**, 160–169.
- 76 V. Lobo, A. Patil, A. Phatak and N. Chandra, *Pharmacognosy Reviews*, 2010, **4**, 118–126.
- 77 C. E. Brubaker, H. Kissler, L. J. Wang, D. B. Kaufman and P. B. Messersmith, *Biomaterials*, 2009, **31**, 420–427.
- 78 C. Lee, J. Shin, J. S. Lee, E. Byun, J. H. Ryu, S. H. Um, D. I. Kim, H. Lee and S. W. Cho, *Biomacromolecules*, 2013, **14**, 2004–2013.
- 79 S. Hong, K. Yang, B. Kang, C. Lee, I. T. Song, E. Byun, K. I. Park, S.-W. W. Cho and H. Lee, *Advanced Functional Materials*, 2013, **23**, 1774–1780.
- 80 H. J. Park, Y. Jin, J. Shin, K. Yang, C. Lee, H. S. Yang and S. W. Cho, *Biomacromolecules*, 2016, **17**, 1939–1948.
- 81 J. Shin, J. S. Lee, C. Lee, H.-J. J. Park, K. Yang, Y. Jin, J. H. Ryu, K. S. Hong, S.-H. H. Moon, H.-M. M. Chung, H. S. Yang, S. H. Um, J.-W. W. Oh, D.-I. I. Kim, H. Lee and S.-W. W. Cho, *Advanced Functional Materials*, 2015, **25**, 3814–3824.
- 82 Y. Liang, X. Zhao, P. X. Ma, B. Guo, Y. Du and X. Han, *Journal of Colloid and Interface Science*, 2019, **536**, 224–234.
- 83 L. Wang, Y. Li, L. Lin, R. Mu and J. Pang, *Carbohydrate Polymers*, 2020, **236**, 116045.
- 84 C. Yu, F. Yao and J. Li, *Acta Biomaterialia*, 2021.